

## Muons in gamma showers

M. Drees and F. Halzen

*Physics Department, University of Wisconsin, Madison, Wisconsin 53706*

K. Hikasa

*National Laboratory for High Energy Physics (KEK), Tsukuba, Ibaraki 305, Japan*

(Received 13 June 1988)

We reconsider the calculation of the relative abundance of muons in photon- and proton-induced air cascades. The calculation is relevant to the performance of a new generation of cosmic-ray telescopes presently in the planning or construction stage. We first solve the one-dimensional cascade equations analytically for a power photon spectrum as well as for individual showers. The formalism allows the consideration of physics issues without reliance on electromagnetic cascade Monte Carlo simulation and brings to the forefront several ambiguities in the high-energy calculation. The relative abundance of high-energy particles in a flatter (e.g.,  $E^{-2}$ ) source spectrum can result in similar muon content of photon and hadron showers even with  $\gamma N \rightarrow \pi(\rightarrow \mu\nu)X$  photoproduction cross sections of order 1 mb. A high-energy photoproduction cross section of this magnitude does not necessarily require new physics and can conceivably result from the QCD gluon structure of a high-energy photon.

### I. INTRODUCTION

The discovery of very-high-energy point sources<sup>1</sup> in the cosmic-ray spectrum has inspired a flurry of activity in the construction or planning of future directional cosmic-ray telescopes. The experimental challenge is twofold: (i) With angular resolution of order 1 degree the flux from a cosmic  $\gamma$ -ray accelerator is drowned in the continuous cosmic-ray background except for some sporadic short time bursts of increased emission; (ii) on-source  $\gamma$  showers are very similar in structure to cosmic-ray background showers and it is therefore difficult to explore differences in shower structure to enhance the signal-to-noise ratio. Only the muon content of the observed showers could be qualitatively different between  $\gamma$ - and hadron-induced showers and second-generation experiments have been designed to explore this difference.

At first sight the difference in muon content is guaranteed. In hadron showers the produced charged pions are the source of muons via  $\pi \rightarrow \mu\nu$  decay. A photon-induced electromagnetic shower proceeds by electron pair production and bremsstrahlung and only develops a muon component via processes characterized by very small cross sections relative to the pair-production cross section, which is 500 mb in air. The dominant source of muons in photon showers is pion photoproduction followed by decay of the charged pions, but at higher energies charm photoproduction and muon pair production by photons can also play a role. Standard Monte Carlo implementation<sup>2</sup> of these ideas leads to the result that the number of muons in a photon shower is typically a few percent of the corresponding number in a proton-induced shower of the same energy. This ratio depends weakly on the primary energy of the shower as well as on the muon energy.

As far as we are aware, no high-energy cosmic-ray experiment has ever provided evidenced for the existence of two types of showers differing in muon content by roughly a factor of 30, neither in the cosmic-ray flux nor in the beam emitted by cosmic accelerators. Any experiment trying to identify the lower muon content of showers from point sources has failed to do so.<sup>3</sup> Underground muon signals from point sources are also consistent with the expected flux if photon showers are indeed muon poor. One must wonder what the implications are for decades of cosmic-ray observations if one suddenly declares that the electromagnetic and hadronic parts of the cascades have similar muon content. The question has been raised and answered by Hillas<sup>4</sup> and if anything, a better fit is obtained to a wide set of high-energy air-shower information. Given the crucial role muons play in the next round of experiments, it is imperative to reconsider the calculation independently of whether the "muon puzzle" survives further scrutiny.

The standard calculation<sup>2,5,6</sup> of muons in  $\gamma$ -ray showers follows a familiar road: one fits accelerator data on pion photoproduction with a functional form incorporating some slow logarithmic increase of the cross section with energy and incorporates the process in a standard electromagnetic Monte Carlo simulation. This is also the way hadronic showers have been studied in the past and we have learned recently that such a procedure is totally inadequate to attack the TeV region and above.<sup>7</sup> The reason is that the QCD structure of very-high-energy interactions implies features that cannot be represented by simple logarithmic extrapolation of low-energy accelerator data. The physics reason is easy to trace by computing the cross section of producing a jet of transverse momentum  $> p_{T_{\min}}$  in a gluon-gluon collision through which two hadrons interact:

$$\sigma_{\text{jet}} = \int_{p_{T\text{min}}} dp_T^2 \int dx_1 dx_2 g(x_1)g(x_2) \frac{d\hat{\sigma}}{dp_T^2}, \quad (1.1)$$

where

$$\frac{d\hat{\sigma}}{dp_T^2}(gg \rightarrow gg) \simeq \frac{9\pi\alpha_s^2}{2p_T^4}. \quad (1.2)$$

For a toy gluon structure function  $g(x) = 3(1-x)^5/x$  and  $\alpha_s \simeq 0.2$  we obtain, from (1.1), (1.2), and for  $p_{T\text{min}} \simeq 1$  GeV and  $\sqrt{s} \simeq 1$  TeV,

$$\sigma_{\text{jet}} \simeq 80 \text{ mb}. \quad (1.3)$$

This jet cross section is of order of the total cross section and therefore at high energy where the gluon structure is fully developed, hadron collisions become perturbative or semihard. The fact that a 1-GeV gluon jet cannot be resolved in an experiment is irrelevant. The phenomenon described above, where hadron collisions move from a regime where the valence quarks dominate the interaction to a regime where large numbers of relative soft gluons dictate the structure of high-energy interactions, has in fact all the features of a threshold in the  $E \simeq 10$  TeV energy range.<sup>7</sup> Average high-energy collisions contain semihard gluon interactions and this jetty behavior is first revealed by the minijet data of the UA1 experiment.<sup>8</sup> It is well known that all emulsion events in excess of 100 TeV have a multiple-core structure. It has also been argued that the violation of Feynman and Koba-Nielsen-Olesen (KNO) scaling as well as a plethora of other phenomena<sup>9</sup> in the 10–100-TeV energy region are features of this rapid change from quark to gluon dominance of hadron interactions. These include the increase with energy of the average transverse momentum, the correlation between  $\langle p_T \rangle$  and multiplicity, the higher multiplicity of strange particles, and, more speculatively, the rise of the total cross section and of the real-to-imaginary part of the forward amplitude with energy. It is an understatement to say that standard Monte Carlo simulations do not represent the physics of the interactions as dictated by QCD. A program is underway to remedy this situation.<sup>10</sup>

Drees and Halzen pointed out<sup>11</sup> that a corresponding threshold can result in large photoproduction cross sections once the photon develops a significant gluon structure function. The diagram is shown in Fig. 1 and the

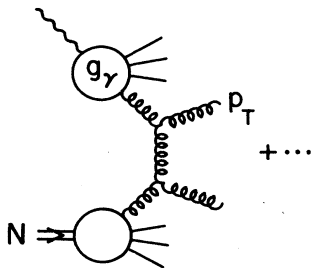


FIG. 1. Typical diagram representing the photoproduction of hadrons mediated by the gluon structure function of the photon.

corresponding cross section is calculated in analogy to Eq. (1.1):

$$\sigma_{\gamma N} = \int_{p_{T\text{min}}} dp_T^2 \int dx_1 dx_2 g_\gamma(x_1)g(x_2) \frac{d\hat{\sigma}}{dp_T^2}. \quad (1.4)$$

Here  $g_\gamma$  is the gluon structure function of the photon. The high-energy value of the cross section is again dominated by  $gg \rightarrow gg$  scattering and the predicted photoproduction cross section<sup>12</sup> at 1000 TeV is shown for a range of minimum jet transverse momenta in Fig. 2. Cross sections of order 1 mb (and not the canonical 100  $\mu\text{b}$  observed at accelerators) are anticipated in QCD as the photoproduction rate is  $O(\alpha/\alpha_s)$  and not  $O(\alpha)$  relative to the hadronic cross section as naively expected. This is obvious from comparison of Eqs. (1.1) and (1.4); the photoproduction of gluons is  $O(\alpha\alpha_s)$ , whereas gluon hadroproduction is  $O(\alpha_s^2)$ . Notice also that these calculations should be reliable provided  $p_T \gg \Lambda_{\text{QCD}}$ . It is a fact<sup>8</sup> that the calculation (1.1) adequately represents jet data in  $p\bar{p}$  interactions for  $p_T \gtrsim 3$  GeV. For the rapid rise of the jet cross section to drive the increase of the total cross section, minimum  $p_T$  values of 1–2 GeV are required.<sup>9</sup> It is therefore reasonable to explore the photoproduction of pions via gluons in the photon for this range of  $p_T$  values as is done in Fig. 2. The value of the cross section can be determined in the near future at the DESY  $ep$  collider HERA at  $E \lesssim 50$  TeV using photons radiated by the electron beam.<sup>11</sup>

The aim of this paper is twofold: (i) We present analytical methods to perform a calculation of the muon flux from a power photon spectrum and from an individual high-energy photon; and (ii) we present explicit estimates for a range of photoproduction cross sections. Having analytic one-dimensional solutions to the cascade equations has several advantages. It reveals aspects of the problem not transparent in a Monte Carlo calculation and will allow anyone to experiment with physics ideas without having to face the use of an electromagnetic-

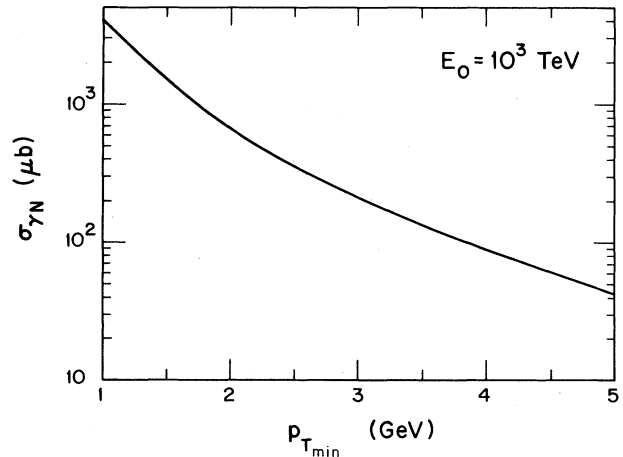


FIG. 2. Photoproduction cross section at  $10^3$  TeV energy as a function of the minimum transverse momentum of the produced jet defined in Eq. (1.4). Calculations are taken from Ref. 11.

shower simulation program. We subsequently experiment ourselves with the QCD ideas just introduced. Our tentative conclusion is that the prediction of the muon content of electromagnetic cascades is more flexible than previously anticipated. The analytic methods clearly display the possibility of getting large muon rates with relatively modest photoproduction cross sections provided the source has an  $E^{-2}$  or flatter spectrum.

## II. MUONS IN PHOTON-INDUCED SHOWERS: POWER SPECTRUM

We first calculate muons from pions photoproduced by photon-induced showers from a point source. For the primary photon spectrum we assume

$$\frac{dN_\gamma}{dE}(E, t=0) = \frac{a}{E^2}, \quad (2.1)$$

as suggested<sup>1</sup> by data from Cygnus X-3 as a typical example. Equation (2.1) represents the source flux at the top of the atmosphere ( $t=0$ ). Depth in the atmosphere is defined in column density in  $\text{g}/\text{cm}^2$ . For a  $E^{-2}$  spectrum the photon spectrum inside the atmosphere is essentially independent of depth:<sup>13</sup>

$$\frac{dN_\gamma}{dE}(E, t) \equiv \gamma(E, t) = \frac{a}{2E^2}. \quad (2.2)$$

In the atmospheric cascade, pions are generated by the photoproduction process in the interaction of photons in the cascade (2.2) with air nuclei (nitrogen-oxygen mixture with average  $A=14.5$ ). The linear cascade equation<sup>13,6</sup> for the flux of pions is

$$\begin{aligned} \frac{d\pi}{dt} = & \left[ -\frac{1}{\lambda_\pi} - \frac{1}{d_\pi} \right] \pi \\ & + \int_0^1 \frac{dx}{x} \frac{\pi(E/x, t)}{\lambda_\pi} \left[ \frac{1}{\sigma_{\pi N}} \frac{d\sigma_{\pi \rightarrow \pi}(x)}{dx} \right] \\ & + \int_0^1 \frac{dx}{x} \frac{\gamma(E/x, t)}{\lambda_{\gamma N}} \left[ \frac{1}{\sigma_{\gamma N}} \frac{d\sigma_{\gamma \rightarrow \pi}(x)}{dx} \right]. \end{aligned} \quad (2.3)$$

The first term represents the depletion of  $\pi$  by interaction (interaction length  $\lambda_\pi$ ) and decay (decay length  $d_\pi$ ) with increasing depth. The second term takes into account the regeneration of  $\pi$  by higher-energy pions with  $E'=E/x$  interacting with air nuclei. Finally, the last term represents the generation of  $\pi$  by photoproduction  $\gamma N \rightarrow \pi X$  with cross section  $\sigma_{\gamma N}$ . We use the standard definition of radiation, interaction, and decay length (defined for convenience in terms of column density) with<sup>14</sup>

$$d_\pi = t \frac{E \cos \theta}{\epsilon_\pi}, \quad (2.4)$$

assuming an exponential density distribution of the atmosphere. Here  $\theta$  is the zenith angle and  $\epsilon_\pi = m_\pi h_0 / \tau_\pi = 115 \text{ GeV}$  for an average height of the atmosphere at sea level  $h_0 = 6.4 \text{ km}$ . Notice that  $\lambda$  and  $\sigma$  in Eq. (2.3) can in general depend on energy; those under the integration sign are at  $E/x$ .

For TeV pions with  $E \gg \epsilon_\pi \lambda_\pi / t \cos \theta$ , the pion decay is negligible and we can omit the  $1/d_\pi$  term in (2.3). If we further neglect the energy dependence of the  $\gamma N$  and  $\pi N$  cross sections<sup>15</sup> and assume Feynman scaling for the inclusive cross section  $\sigma_{\gamma \rightarrow \pi}$  and  $\sigma_{\pi \rightarrow \pi}$ , Eq. (2.3) can be factorized as follows. We take the ansatz

$$\pi(E, t) = \Gamma_0(E) \pi_2(t) \quad (2.5)$$

with

$$\Gamma_0(E) = \frac{a}{2E^2}. \quad (2.6)$$

Now Eq. (2.3) reduces to

$$\frac{d\pi_2}{dt} = -\frac{1}{\Lambda_\pi} \pi_2 + \frac{z_{\gamma\pi}}{\lambda_{\gamma N}}, \quad (2.7)$$

where

$$\Lambda_\pi = \frac{\lambda_\pi}{1 - z_{\pi\pi}}, \quad (2.8)$$

$$z_{\pi\pi} = \frac{1}{\sigma_{\pi N}} \int_0^1 dx x \frac{d\sigma_{\pi \rightarrow \pi}(x)}{dx}, \quad (2.9)$$

$$z_{\gamma\pi} = \frac{1}{\sigma_{\gamma N}} \int_0^1 dx x \frac{d\sigma_{\gamma \rightarrow \pi}(x)}{dx}. \quad (2.10)$$

$\lambda_{\gamma N}$  is the interaction length associated with  $\pi$  photoproduction and  $\Lambda_\pi (> \lambda_\pi)$  is the effective pion interaction length in the atmosphere because  $\pi$  are regenerated in interactions. This increase depends indeed on  $z_{\pi\pi} = \langle nx \rangle_{\pi\pi}$ , i.e., the average multiplicity  $n$  multiplied by relative momentum  $x$  of pions generated by parent  $\pi$  of energy  $E_\pi/x$ . The solution of (2.7) is

$$\pi_2 = \frac{z_{\gamma\pi}}{\lambda_{\gamma N}} \Lambda_\pi (1 - e^{-t/\Lambda_\pi}) \simeq \frac{z_{\gamma\pi}}{\lambda_{\gamma N}} \Lambda_\pi. \quad (2.11)$$

Equation (2.11) can be used to calculate the flux of high-energy ( $\gtrsim \text{TeV}$ ) muons as will be done shortly. On the other hand, for the derivation of low-energy muon flux, the so-far neglected decay term in Eq. (2.3) becomes dominant. In this case we look for an approximate solution of the form

$$\pi(E, t) = \Gamma_0(E) \pi_2(E, t). \quad (2.12)$$

Inserting (2.12) into (2.3) and neglecting all pion interactions which are irrelevant for low-energy pions gives

$$\frac{d\pi_2(E, t)}{dt} = -\frac{\delta}{t} \pi_2(E, t) + \frac{z_{\gamma\pi}}{\lambda_{\gamma N}} \quad (2.13)$$

with  $\delta = \epsilon_\pi / E \cos \theta$  [see Eq. (2.4)]. The solution of (2.13) is

$$\pi_2 = \frac{z_{\gamma\pi}}{\lambda_{\gamma N}} \int_0^t \left[ \frac{t'}{t} \right]^\delta dt' = \frac{z_{\gamma\pi}}{\lambda_{\gamma N}} \frac{t}{\delta + 1}, \quad (2.14)$$

which becomes the exact solution of Eq. (2.3) in the limit  $t \ll \Lambda_\pi$ . Our final result for the  $\pi$  flux is obtained from (2.11) and (2.14):

$$\pi(E, t) = \Gamma_0(E) \frac{z_{\gamma\pi}}{\lambda_{\gamma N}} \min \left[ \Lambda_\pi \frac{t}{\delta + 1} \right]. \quad (2.15)$$

The muon spectrum is obtained by folding the  $\pi$  spectrum with the two-body decay distribution  $\pi \rightarrow \mu\nu$ :

$$\frac{dN_\mu}{dE dt} = \int_E^{E/r} \frac{dE'}{(1-r)E'} \frac{\pi(E', t)}{d_\pi}, \quad (2.16)$$

where  $r = m_\mu^2/m_\pi^2$ . In the high-energy limit where  $\delta$  in Eq. (2.16) can be neglected, we have

$$\begin{aligned} \frac{dN_\mu}{dE}(E) &= \Gamma_0(E) \frac{\epsilon_\pi}{E \cos\theta} \frac{1-r^3}{3(1-r)} \frac{z_{\gamma\pi}}{\lambda_{\gamma N}} \\ &\times \int_0^{t_{\max}} \frac{dt}{t} \min(\Lambda_\pi t). \end{aligned} \quad (2.17)$$

There is an effective upper limit on the integration in Eq. (2.17) given by the depth  $t_{\max}$  where the photon energy in the cascade has become too low to produce muons of energy  $E$ . The primary photon energy is reduced from  $E_{\max}$  to  $E_{\max}/2^n$  after a depth  $t = n(\ln 2)\lambda_R$ , i.e., the energy is reduced by a factor of 2 for every  $(\ln 2)\lambda_R$  increment in depth, where  $\lambda_R$  is the radiation length. A cosmic accelerator has a maximum energy cutoff<sup>1</sup> on the spectrum (2.1) which we denote by  $E_{\max}$ . No muons of energy  $E$  are produced after a number  $n_{\max}$  of layers determined by

$$\frac{E_{\max}}{2^{n_{\max}}} = \frac{E}{\langle x \rangle_{\gamma \rightarrow \mu}}. \quad (2.18)$$

Here  $E/\langle x \rangle_{\gamma \rightarrow \mu}$  is the  $\gamma$  energy required to produce a muon of energy  $E$ . Therefore,

$$t_{\max} = \lambda_R \ln \left[ \frac{E_{\max} \langle x \rangle_{\gamma \rightarrow \mu}}{E} \right]. \quad (2.19)$$

Explicit integration of (2.17) gives

$$\frac{dN_\mu}{dE} = \Gamma_0(E) \frac{\epsilon_\pi}{E \cos\theta} \frac{1-r^3}{3(1-r)} z_{\gamma\pi} \frac{\Lambda_\pi}{\lambda_{\gamma N}} \left[ 1 + \ln \left[ \frac{t_{\max}}{\Lambda_\pi} \right] \right]. \quad (2.20)$$

For the low-energy solution ( $E_\mu \ll \epsilon_\pi$ ), we have instead

$$\frac{dN_\mu}{dE} = \Gamma_0(E) \frac{1-r^2}{2(1-r)} z_{\gamma\pi} \frac{t_{\max}}{\lambda_{\gamma N}} \quad (2.21)$$

for  $t_{\max} \ll \epsilon_\pi \Lambda_\pi / E \cos\theta$ . The limiting solutions (2.20) and (2.21) may be combined into the interpolation formula

$$\frac{1}{\Gamma_0(E)} \frac{dN_\mu}{dE} = \frac{\Lambda_\pi}{\lambda_{\gamma N}} z_{\gamma\pi} \frac{L_\gamma}{1 + (L_\gamma/H_\gamma)(E \cos\theta/\epsilon_\pi)} \quad (2.22)$$

with

$$L_\gamma = \frac{1-r^2}{2(1-r)} \frac{t_{\max}}{\Lambda_\pi}, \quad (2.23)$$

$$H_\gamma = \frac{1-r^3}{3(1-r)} \left[ 1 + \ln \frac{t_{\max}}{\Lambda_\pi} \right]. \quad (2.24)$$

The formalism presented here is closely patterned after the calculation of the muon spectrum induced by primary hadronic cosmic rays.<sup>16</sup> The muon content of hadron induced showers can also be expressed in the form (2.22)–(2.24):

$$\frac{1}{N_0(E)} \frac{dN_\mu}{dE} = \frac{\Lambda_N}{\lambda_N} z_{N\pi} \frac{L_N}{1 + (L_N/H_N)(E \cos\theta/\epsilon_\pi)}, \quad (2.25)$$

where  $N_0(E) \sim E^{-(\gamma+1)}$  represents the cosmic-ray flux at the top of the atmosphere and

$$\frac{\Lambda_N}{\lambda_N} = \frac{1}{1-z_{NN}} = \left[ 1 - \frac{1}{\sigma_{NN}} \int_0^1 dx x^\gamma \frac{d\sigma_{N \rightarrow N}}{dx} \right]^{-1}, \quad (2.26)$$

$$L_N = \frac{1}{\gamma+1} \frac{1-r^{\gamma+1}}{1-r}, \quad (2.27)$$

$$H_N = \frac{1}{\gamma+2} \frac{1-r^{\gamma+2}}{1-r} \frac{\Lambda_\pi}{\Lambda_\pi - \Lambda_N} \ln \frac{\Lambda_\pi}{\Lambda_N}. \quad (2.28)$$

Here  $z_{N\pi}$  is defined as in (2.26) and one recognizes the similarity between the result (2.27) and (2.28) for  $\gamma=1$  (i.e., for the  $E^{-2}$  spectrum of  $\gamma$  rays) and (2.23) and (2.24). The formalism presented here will overestimate the muon content of a shower once the muon energy drops below 10 GeV since  $\mu$  decay and  $\mu$  energy loss have not been taken into account. For very-high-energy muons the contribution of  $K$  decay into muons has to be included. The calculation parallels that for  $\pi$  decay.

In order to explore the validity of the formalism we compute the vertical ( $\cos\theta=1$ ) muon intensity  $dN_\mu/dE$  at sea level induced by the cosmic-ray flux of nucleons:

$$N_0(E) = 1.8 \left[ \frac{E}{\text{GeV}/A} \right]^{-2.7} \text{cm}^{-2} \text{sr}^{-1} \text{sec}^{-1} \quad (2.29)$$

from (2.25)–(2.28). For  $\gamma=1.7$ , corresponding to the flux (2.29), accelerator data and (2.26) imply<sup>16</sup>

$$z_{NN} \simeq z_{\pi\pi} \simeq 0.3, \quad (2.30)$$

$$z_{N\pi} \simeq 0.08,$$

and

$$\lambda_\pi = 1.3\lambda_N \simeq 110 \text{ g cm}^{-2} \quad (2.31)$$

in air. The calculated vertical muon intensity at sea level describes the observations<sup>17</sup> remarkably well above  $E=10$  GeV muon energy; see Fig. 3. Below that energy the formalism overestimates the muon yield as anticipated, e.g., by a factor 4 for  $E=4$  GeV, the threshold of the CYGNUS experiment at Los Alamos.<sup>18</sup>

We now turn our attention to muons emitted by a  $\gamma$ -ray source with  $E^{-2}$  spectrum. Cygnus X-3 data are adequately described in the x-ray region and above by (2.1), (2.2) with<sup>1</sup>

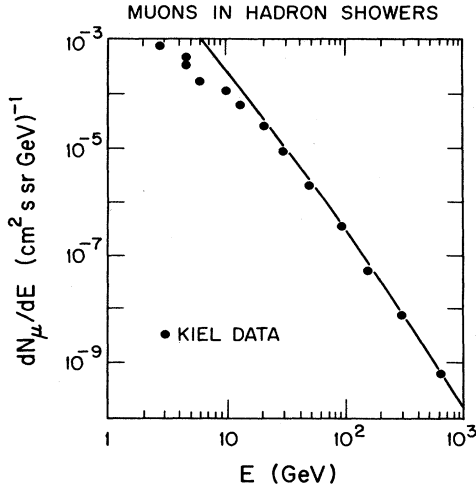


FIG. 3. Illustration of the validity of the analytic techniques used in this paper. Differential spectrum of muons produced by cosmic rays as a function of the muon energy. Calculation using Eq. (2.25), data from Ref. 17.

$$a = 4 \times 10^{-11} \text{ cm}^{-2} \text{ sec}^{-1} \quad (2.32)$$

for  $E$  in TeV units. The spectrum is cut off at  $E_{\text{max}} \approx 10^5$  TeV. Before deriving some explicit results from (2.22)–(2.24), a few general remarks are in order. It is not correct that the photoproduction cross section  $\sigma_{\gamma N}$ , which is  $\sim 100 \mu\text{b}$  at accelerator energies, has to match the hadronic cross section  $\sigma_{NN}$  of  $\sim 100 \text{ mb}$  to spoil the expected suppression of muons in photon relative to proton-induced showers. First, an  $E^{-2}$   $\gamma$  spectrum fills the atmosphere uniformly with high-energy  $\gamma$  rays; i.e.,  $N_\gamma$  is independent of depth  $t$  as seen from (2.2) up to a depth  $t_{\text{max}} = (\ln 2)n_{\text{max}}\lambda_R$  determined by (2.18) and (2.19), which is typically  $(5-15)\lambda_R$ . All these photons can photoproduce  $\pi$  which are the progenitors of the muons. Meanwhile, the nucleon spectrum dies away exponentially as  $\exp(-t/\Lambda_N)$ . This leads to the enhancement factor  $t_{\text{max}}$  for low-energy muons or  $\ln t_{\text{max}}$  for high-energy muons in the flux (2.22). The relative abundance of high-energy particles will also enhance the effect of regeneration of  $\pi$  by  $\pi \rightarrow \pi$  on air nuclei. This is implemented by the change  $\lambda_\pi \rightarrow \Lambda_\pi$  and implies an enhancement factor  $(1 - z_{\pi\pi})^{-1}$ . For a  $\gamma = 1.7$  cosmic-ray spectrum  $z_{\pi\pi} \approx z_{NN} \approx 0.3$ . For  $\gamma = 1$ , the quantity  $z_{\pi\pi}$  could be significantly larger; see Eq. (2.26) with  $N$  replaced by  $\pi$ . For  $\gamma > 1$ , the dominant contribution of the inclusive cross section  $\sigma_{\pi \rightarrow \pi}$  is indeed suppressed by a factor  $x^{\gamma-1}$ . If, e.g.,  $z_{\pi\pi} = \frac{2}{3}$  for a  $\gamma = 1$  spectrum,<sup>19</sup> we have  $\Lambda_\pi = 3\lambda_\pi$  leading to a factor 3 enhancement of  $dN_\mu/dE$  at high energy; see (2.22).

We are now ready to compute the muon yield from a point source such as Cygnus X-3 from (2.22)–(2.24) in conjunction with the flux (2.32). We specifically assume

$$z_{\gamma\pi} = \langle nx \rangle_{\gamma \rightarrow \pi} = \frac{2}{3}, \quad (2.33)$$

$$\frac{\lambda_R}{\lambda_{\gamma N}} = \frac{A\sigma_{\gamma N}}{\sigma_R} = \frac{14.5\sigma_{\gamma N}(\text{mb})}{480}, \quad (2.34)$$

$$\frac{\lambda_R}{\Lambda_\pi} = (1 - z_{\pi\pi}) \frac{A\sigma_{\pi N}}{\sigma_R} \approx 0.4(1 - z_{\pi\pi}). \quad (2.35)$$

Here we took 480 mb for the dominant Bethe-Heitler cross section  $\sigma_R$  of photons on air and assumed that  $\frac{2}{3}$  of the energy  $\langle nx \rangle$  of photoproduced  $\pi$  goes into  $\pi^\pm$  and therefore into potential progenitors of muons. In the calculation of  $t_{\text{max}}$  from (2.19) we assume  $\langle x \rangle_{\gamma \rightarrow \mu} = 0.25$  but the results are insensitive to the precise value. The standard Monte Carlo results<sup>2</sup> can be reproduced within errors by Eq. (2.22) assuming a photoproduction cross section  $\sigma_{\gamma N} = 100 \mu\text{b}$  and  $z_{\pi\pi} = 0.3$ ; see Fig. 4. This value of  $\sigma_{\gamma N}$  represents a typical high-energy cross section measured at accelerator energies. Notice that the “standard” Monte Carlo results could easily be boosted by a factor as a result of the larger value of  $z_{\pi\pi}$  for a  $\gamma = 1$  spectrum. We remind the reader at this point of the result of Stanev, Gaisser, and Halzen<sup>2</sup> that a factor 3 in photoproduction rate (e.g.,  $z_{\pi\pi} = \frac{2}{3}$ ) is sufficient to accommodate the muon excess in the showers from Cygnus X-3 in the Kiel experiment<sup>20</sup> by punchthrough in the 2-m slab of concrete absorber used to identify “muons.” We also show in Fig. 4 a calculation of the muon content of  $\gamma$  showers for an increased photoproduction cross section  $\sigma_{\gamma N} = 1 \text{ mb}$  and  $z_{\pi\pi} = \frac{2}{3}$ . Such values could conceivably result from the high-energy photon interacting with matter via its gluon structure function;<sup>21</sup> see Fig. 2. Muon yields in excess by 1–2 orders of magnitudes of the “standard” prediction are obtained.

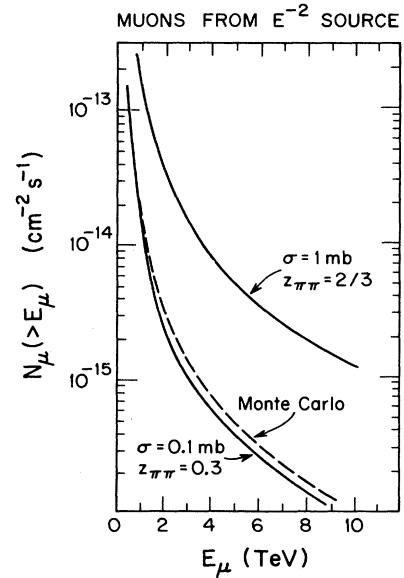


FIG. 4. Integral spectrum of muons produced by a Cygnus-like point source with photon spectrum (2.1) calculated from Eq. (2.22) for two choices of the photoproduction cross section  $\sigma$  and  $z_{\pi\pi}$ . Also shown is the result of the Monte Carlo calculation of Ref. 6 which also assumed a 0.1-mb photoproduction cross section.

### III. PHOTON-INDUCED SHOWER: SINGLE SHOWER

If one is interested in the development of a single photon shower, one is to solve Eq. (2.3) with the initial condition

$$\gamma(E,0) = \delta(E - E_0). \quad (3.1)$$

As it is not possible to solve the equation analytically, we consider the following discrete approximation<sup>13</sup> where the atmosphere is segmented in layers of depth  $(\ln 2)\lambda_R$  over which electromagnetic particles lose half their energy.

(1) At depth  $t = n(\ln 2)\lambda_R$ , the shower consists of  $2^n/3$  photons (and the same number of electrons and positrons) of energy  $E_0/2^n$ . (2) A photon at layer  $n$  produces  $(\lambda_R/\lambda_{\gamma N})\langle n_{\gamma\pi} \rangle$  pions of energy  $(E_0/2^n) \cdot \langle x_{\gamma\pi} \rangle$ . (3) The number of muons with energy  $> E_\mu^0$  produced by a pion is  $[\min(\lambda_\pi/d_\pi, 1)]P(E_\mu^0; E_\pi)$ . Here  $P(E_\mu^0; E_\pi)$  is the probability that a pion of energy  $E_\pi$  decays into a muon of energy greater than  $E_\mu^0$ :

$$P(E_\mu^0; E_\pi) = \begin{cases} 0, & E_\pi < E_\mu^0, \\ \frac{E_\pi - E_\mu^0}{(1-r)E_\pi}, & E_\mu^0 < E_\pi < E_\mu^0/r, \\ 1, & E_\pi > E_\mu^0/r. \end{cases} \quad (3.2)$$

For high-energy muons we have  $\lambda_\pi/d_\pi = \lambda_\pi \epsilon_\pi / E_\pi n(\ln 2)\lambda_R \cos\theta \ll 1$  for the relevant pion energies and the total number of muons is obtained by summing over  $n$  layers of atmosphere from  $n = 1$  to  $n_{\max}$ :

$$\begin{aligned} N_\mu(E > E_\mu^0) &= \sum_{n=1}^{n_{\max}} \frac{2^n}{3} \frac{\lambda_R}{\lambda_{\gamma N}} \langle n_{\gamma\pi} \rangle \frac{2^n \lambda_\pi \epsilon_\pi}{E_0 \langle x_{\gamma\pi} \rangle n(\ln 2)\lambda_R \cos\theta} \\ &= \frac{1}{3} \left[ \sum_{n=1}^{n_{\max}} \frac{2^{2n}}{n} \right] \frac{\epsilon_\pi}{E_0 \cos\theta} \frac{1}{(\ln 2)} \frac{\lambda_\pi}{\lambda_{\gamma N}} \frac{\langle n_{\gamma\pi} \rangle}{\langle x_{\gamma\pi} \rangle} \\ &= \frac{2}{3} \frac{2^{2n_{\max}}}{n_{\max}} \frac{\epsilon_\pi}{E_0 \cos\theta} \frac{\lambda_\pi}{\lambda_{\gamma N}} \frac{\langle n_{\gamma\pi} \rangle}{\langle x_{\gamma\pi} \rangle}, \end{aligned} \quad (3.3)$$

where the final expression is the approximate form for the range of  $n_{\max}$  of interest, and  $n_{\max}$  is the effective number of layers which can produce muons of energy  $> E_\mu^0$ . It is given by

$$n_{\max} = \ln \frac{\eta E_0 \langle x_{\gamma\pi} \rangle}{E_\mu^0} / \ln 2, \quad (3.4)$$

where  $\eta$  is a number between  $r$  and 1. Equation (3.3) can be rewritten as

$$N_\mu(E > E_\mu^0) = \frac{2}{3n_{\max}} \eta^2 \frac{\epsilon_\pi E_0}{(E_\mu^0)^2 \cos\theta} \frac{\Lambda_\pi}{\lambda_{\gamma N}} \langle n_{\gamma\pi} \rangle \langle x_{\gamma\pi} \rangle, \quad (3.5)$$

where we have replaced  $\lambda_\pi$  by  $\Lambda_\pi$  to take into account the effect of secondary pions from pion interactions with nuclei. We determine  $\eta$  by requiring consistency of the above result convoluted with a primary power spectrum

with the analytic result obtained previously (2.20):

$$\eta^2 \simeq \frac{1-r^3}{4(1-r)} \frac{1}{1.4} \simeq 0.34. \quad (3.6)$$

In deriving (3.6) notice that  $z_{\gamma\pi} = \langle n_{\gamma\pi} x_{\gamma\pi} \rangle$ .

We next illustrate (3.5) and (3.6) for some specific examples. We can write (3.5) in the form

$$\begin{aligned} N_\mu(E > E_\mu^0) &= \frac{1}{n_{\max}} \frac{0.23}{\cos\theta} \frac{\epsilon_\pi E_0}{(E_\mu^0)^2} \frac{1}{1-z_{\pi\pi}} \frac{A \sigma_{\gamma N}}{\sigma_{\pi A}} \\ &\times \langle nx \rangle_{\gamma \rightarrow \pi}. \end{aligned} \quad (3.7)$$

We fix all inputs as before:

$$\begin{aligned} \epsilon_\pi &= 115 \text{ GeV}, \\ \frac{1}{3} &\lesssim z_{\pi\pi} \lesssim \frac{2}{3}, \\ \sigma_{\pi A} &= 198 \text{ mb}, \\ \langle nx \rangle_{\gamma \rightarrow \pi^\pm} &= \frac{2}{3}, \\ \langle x \rangle_{\gamma\pi} &= \frac{1}{4} \end{aligned} \quad (3.8)$$

(precise values are not important) and study  $N_\mu$  as a function of the photoproduction cross section  $\sigma_{\gamma N}$ . In Table I we compare the results of (3.7) and (3.8) with the Stanev, Gaisser, and Halzen<sup>2</sup> Monte Carlo simulation for a photon with primary energy  $E_0 = 10^3$  TeV. As was the case for the  $E^{-2}$  spectrum, the Monte Carlo results are adequately reproduced for  $\sigma_{\gamma N} = 100 \mu\text{b}$  and  $z_{\pi\pi} = 0.3$ . The result is also shown in Fig. 5 along with a calculation assuming  $\sigma_{\gamma N} = 1 \text{ mb}$ ,  $z_{\pi\pi} = \frac{2}{3}$  as could be expected from photoproduction of  $\pi$  via the gluon structure of the pho-

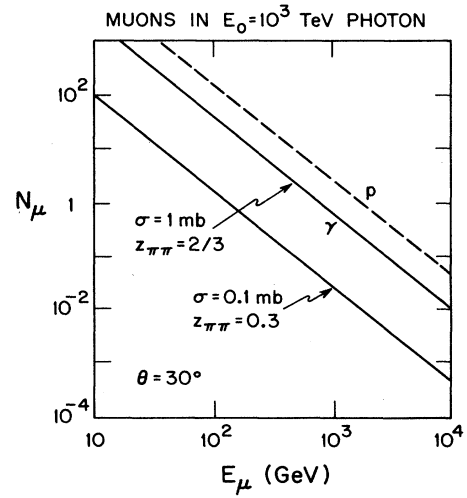


FIG. 5. Number of muons in a  $10^3$ -TeV photon shower for a  $30^\circ$  zenith angle calculated from Eq. (3.7) for two choices of the photoproduction cross section  $\sigma$  and  $z_{\pi\pi}$ . The number of muons in a proton shower of the same energy is shown for comparison.

TABLE I. Muons in  $E_0 = 10^3$  TeV photon shower with conventional photon interactions with nuclei.

$E_\mu$	Monte Carlo simulation (Ref. 2)	Approx. result [Eq. (3.7)]
4 TeV	$3.1 \times 10^{-3}$	$2.2 \times 10^{-3}$
1 TeV	$1.4 \times 10^{-2}$	$2.6 \times 10^{-2}$
0.25 TeV	$6.5 \times 10^{-1}$	$3.3 \times 10^{-1}$
16 GeV	40	55

ton. A parametrization<sup>16</sup> of the muon content of proton showers

$$N_\mu^p(E > E_\mu) = \frac{1.4 \times 10^{-2}}{\cos\theta E_\mu (\text{TeV})} \left( \frac{E_0}{E_\mu} \right)^{0.757} \quad (3.9)$$

is shown for comparison. At this energy QED pair production of muons and leptonic decay of photoproduced charmed particles will further enhance the muon content of the shower. Explicit calculations can be found in Halzen, Hikasa, and Stanev.<sup>6</sup> In the QCD scenario, similar muon content of very-high-energy  $\gamma$  and proton showers can therefore be contemplated.

#### IV. CONCLUSIONS

We have performed an explicit calculation of the muon content of individual photon showers and of the air cascade generated by an  $E^{-2}$  photon spectrum. By avoiding Monte Carlo techniques, the physics issues involved in the calculation are more clearly exhibited. Our formalism also provides a laboratory for experimenting with different assumptions and new physics ideas. The formalism is approximate and has shortcomings. For instance, the results for individual showers depend on  $z_{\pi\pi}$  which depends on the spectral index  $\gamma$ . This is clearly an artifact of our procedure to normalize  $\eta$  in Eq. (3.6). Nev-

ertheless, the one-dimensional shower formalism reproduces all Monte Carlo results within reasonable errors provided the photon and muon energies are not too low. Our goal is not to speculate on the various anomalies scattered over the literature, but to point out that the ambiguities in doing the calculations far above accelerator energies could be larger than previously anticipated. The reason is that cross sections have nontrivial energy dependence in the 10–100-TeV energy region associated with the gluon structure of hadrons. This is by now an experimental fact for hadron-hadron cross sections and it could very well also lead to photoproduction cross sections with characteristics not apparent as present accelerators. The DESY  $ep$  collider HERA could play an important role in elucidating the structure of photoproduction at high energies.

*Note added in proof.* In Sec. III a constant photon-nucleon cross section is assumed. If there is a drastic increase in the cross section in the TeV region as suggested in Ref. 11, the description is not appropriate for GeV muons as opposed to TeV muons. We may improve our formula (3.3) by introducing a step-function approximation for the cross section with a threshold energy  $E_{th}$  of order of TeV. In that case, the number of muons may be written as a sum of the conventional contribution [Eq. (3.5) with the low-energy cross section] and the “new-physics” contribution, which is equal to the last line of Eq. (3.3) with the large cross section, but  $E_\mu^0$  in  $n_{max}$  should be replaced by  $E_{th}$ . This modification reduces the number of muons in the GeV region in Fig. 5.

#### ACKNOWLEDGMENTS

This research was supported in part by the University of Wisconsin Research Committee with funds granted by the Wisconsin Alumni Research Foundation, and in part by the U.S. Department of Energy under Contract No. DE-AC02-76ER00881. The work of K.H. was supported in part by the Japan Society for the Promotion of Science.

<sup>1</sup>For reviews, see R. Protheroe, in *Proceedings of the 20th International Cosmic Ray Conference*, Moscow, 1987, edited by V. A. Kozyrivsky *et al.* (Nauka, Moscow, 1987), Vol. 8; F. Halzen, in *Probing the Standard Model*, proceedings of the Fourteenth SLAC Summer Institute on Particle Physics, Stanford, California, 1986, edited by E. C. Brennan (SLAC Report No. 312, Stanford, 1987), p. 607.

<sup>2</sup>T. Stanev, T. K. Gaisser, and F. Halzen, *Phys. Rev. D* **32**, 1244 (1985).

<sup>3</sup>Only the Akeno experiment has analyzed data with a cut on muon content. They have, however, never analyzed data without this cut and it is interesting to notice that their observed flux on Cygnus X-3 was low compared to other observations made at the same time (see Ref. 1).

<sup>4</sup>M. Hillas, in *Proceedings of the 19th International Cosmic Ray Conference*, La Jolla, California, 1985, edited by F. C. Jones, J. Adams, and J. C. Mason (NASA Conf. Publ. No. 2876) (Goddard Space Flight Center, Greenbelt, MD, 1985), Vol. 9,

p. 407.

<sup>5</sup>T. Stanev and Ch. P. Vankov, *Phys. Lett.* **158B**, 75 (1985); T. Stanev, Ch. P. Vankov, and F. Halzen, in *Proceedings of the 19th International Cosmic Ray Conference* (Ref. 4), Vol. 7, p. 219.

<sup>6</sup>F. Halzen, K. Hikasa, and T. Stanev, *Phys. Rev. D* **34**, 2061 (1986).

<sup>7</sup>F. Halzen and T. K. Gaisser, *Phys. Rev. Lett.* **54**, 1754 (1985);

<sup>8</sup>UA1 Collaboration, C. Albajar *et al.*, *Nucl. Phys.* **B309**, 405 (1988).

<sup>9</sup>For a review, see J. Rushbrooke, in *Proceedings of the International Europhysics Conference on High Energy Physics*, Bari, Italy, 1985, edited by L. Nitti and G. Preparata (Laterza, Bari, 1986), p. 839; F. Halzen and C. S. Kim, in *Results and Perspectives on Particles Physics*, proceedings of the Rencontre de Physique, La Thuile, Aosta, Italy, 1987, edited by M. Greco (Editions Frontières, Gif-sur-Yvette, France, 1987), p. 135.

- <sup>10</sup>T. K. Gaisser and T. Stanev, Bartol Report No. BA-88-48, 1988 (unpublished).
- <sup>11</sup>M. Drees and F. Halzen, *Phys. Rev. Lett.* **61**, 275 (1988).
- <sup>12</sup>The photon can also couple directly to the partons in the proton. At the energies considered, this mechanism results in a cross section which is at most a 10% correction to the results. It is at present an open question whether the large increase with energy of the jet cross section defined by Eq. (1.1) is indeed the origin of the rise of the total cross section in hadron collisions. See F. Halzen and C. S. Kim, in *Results and Perspective in Particle Physics* (Ref. 9).
- <sup>13</sup>See, e.g., B. Rossi, *High-Energy Particles* (Prentice-Hall, Englewood Cliffs, NJ, 1952).
- <sup>14</sup>Note that  $\lambda_\pi \sigma_\pi = 2.4 \times 10^4$  where  $\lambda_\pi$  is in g/cm<sup>2</sup> and  $\sigma_\pi$  in mb.
- <sup>15</sup>The assumption of scaling is a good approximation for conventional cross sections with logarithmic variation. It may not be so at very high energies, where the cross section may grow faster than logarithmically. The rapid rise of the cross section may be incorporated by introducing an effective threshold energy for the interaction.
- <sup>16</sup>See, e.g., T. K. Gaisser, *Cosmic Rays and Particle Physics* (Cambridge University Press, Cambridge, England, in press).
- <sup>17</sup>O. C. Allkofer *et al.*, in *Proceedings of the 12th International Conference on Cosmic Rays*, Hobart, Tasmania, 1971, edited by A. G. Fenton and K. B. Fenton (University of Tasmania Press, Tasmania, 1971), Vol. 4, p. 1319.
- <sup>18</sup>B. L. Dingus *et al.*, *Phys. Rev. Lett.* **60**, 1785 (1988); **61**, 1906 (1988).
- <sup>19</sup>For a  $\gamma=1$  spectrum momentum conservation implies that  $\sum_j z_{ij} = 1$ ; hence  $z_{\pi\pi} = \frac{2}{3}$  if we neglect particles other than pions and assume isospin symmetry (only charged pions are relevant). The leading-particle effect can further increase the value.
- <sup>20</sup>M. Samorski and W. Stamm, *Astrophys. J.* **268**, L17 (1983).
- <sup>21</sup>The possibility that a large photonuclear cross section can enhance the muon flux was studied, although without underlying physics model, by W. Ochs and L. Stodolsky, *Phys. Rev. D* **33**, 1247 (1986).